 CMC, vol.19, no.1, pp.1-16, 2010

Application of Cosserat Theory to the Modelling of Reinforced Carbon Nananotube Beams

Veturia Chiroiu[1], **Ligia Munteanu**[2] **and Antonio S. Gliozzi**[3]

Abstract: This paper develops a mechanical model for multifunctional reinforced carbon nanotube (CNT) beams. The model is obtained by introducing the couple stresses into the constitutive equations of linear viscoelastic theory. The material functions are determined using the homogenization method.

Keywords: Cosserat theory, viscoelasticity, carbon nanotube films, homogenization method.

1 Introduction

Traditionally viscoelastic and elastomeric materials are used for damping treatment [Liao and Wang (1997); Brackbill, Ruhl, Lesieutre and Smith (2000)]. Although the integration of these materials into composites experiences good energy dissipation, the structural integrity of such composites presents significant challenges. For example, viscoelastic and elastomeric materials cannot be used to reinforce the stiffness/strength of a composite because of the large strains needed in the film to create damping, which requires a soft material. In addition, damping films exhibit a loss in performance at high temperatures (above 60°C) due to the resin penetration and poor thermal stability of the viscoelastic polymer [Biggerstaff and Kosmatka (1998); Biggerstaff and Kosmatka (1998)].

In order to overcome these limitations, carbon nanotubes have been studied extensively in relation to high strength components for reinforced nanocomposites [Srivastava and Atluri (2002); Brenner, Shenderova, Areshkin, Schall and Frankland (2002); Shen and Atluri (2004); Munteanu and Chiroiu (2009)]. Carbon nanotubes have an extremely small size and low density, a very high elastic modulus (>1 TPa), the electric current carrying capacity of order $10^{11} - 10^{12}$A / cm^2 and a very high

[1] Institute of Solid Mechanics of Romanian Academy, Ctin Mille 15, 010141 Bucharest
[2] Institute of Solid Mechanics of Romanian Academy, Ctin Mille 15, 010141 Bucharest
[3] Politecnico of Torino, Physics and Structural Eng. Dept., Corso Duca degli Abruzzi 24, Torino 10129

specific surface area with the aspect ratio of order 10^3 [Calvert (1992); Robertson (1993); Overney (1993); Chiroiu, Munteanu and Donescu (2006)]. The mechanical properties of carbon nanotubes are size dependent with respect to various dimensions and geometries [Theodosiou and Saravanos (2007); Chen, Cheng and Hsu (2007); Solano, Costales, Francisco, Pendáas, Blanco, Lau, He and Pandey (2008); Giannopoulos, Georgantzinos, Katsareas and Anifantis (2010)]. The dependency on the size of the carbon nanotube of the dispersive characteristics and group velocities have been studied by Xie and Long (2006)). The spreading of intershell distances and the inlayer van der Waals interactions in carbon nanotubes depends on the size of the tube [Brenner, Shenderova, Areshkin, Schall and Frankland (2002); Srivastava and Atluri (2002); Nair, Farkas and Kriz (2008); Cheng, Hsu and Chen (2009)]. The importance of the interatomic potentials relies on simplifications of the quantum mechanics and ab initio complexity. These simplifications are very important once they can provide analytical solutions of materials properties [Chakrabarty and Cagin (2008)].

So far, a few continuum mechanics methods have been adopted for studying the carbon nanotubes [Ru (2001); Li and Chou (2003); Nasdala, Ernst, Lengnick and Rothert (2005); Teodorescu, Munteanu, Chiroiu, Dumitriu and Beldiman (2008); Chiroiu, Munteanu, Paun and Teodorescu (2009)]. The necessity for Cosserat theories [Voigt (1887); Cosserat (1909)] originates in the inability of classical theories to account for modelling the deformation processes associated with anisotropic deformable solids with consideration of their rheonomic properties [Pobedria (1998), (1997); Pobedria and Omarov (2007a)]. In the generalized Cosserat theory, the couple-stresses are introduced together with the classical stress tensor. In this context, to the displacement vector, the rotation vector (spin-vector) is attached.

In this paper, a reinforced carbon nanotube beam is studied by using the generalized Cosserat theory. The effective material functions are calculated from the relaxation tensors using the homogenization method. The results obtained via the proposed method are compared with the bending experimental results reported by Koratkar *et al.* (2003).

2 The generalized Cosserat theory

The paper focuses on a nanocomposite beam obtained by introducing a nanofilm interlayer between the plies of the composite. The concept of this nanocomposite was introduced by Koratkar, Wei and Ajayan in 2003. It involves integrating light weight, minimally intrusive nanotube films, composed of densely packed highly interconnected networks of multiwalled carbon nanotube into the interlamina interfaces of the host composite. The nanofilm and epoxy filler interlayer is stacked in between a piezoelectric (PZT-5H) and a Silica sheet. The piezoelectric sheet was

selected since it provided a convenient mechanism (via induced-strain actuation) for exciting the beam modal dynamics. Silica was chosen for the sandwich beam since it can conveniently serve as a foundation for anchoring the nanotube film.

Consider that the sandwich beam occupies a volume $V \subset R^3$ and let Σ_1 and Σ_2 be parts of the surface enclosing the volume$V$. The thicknesses of the silica sheet, nanofilm and piezoelectric sheet are denoted byh_1,h_2 and h_3, respectively. The cross-sectional dimensions of the beam are $(a \times b)$, where $b = h_1 + h_2 + h_3$, while its length is $L \gg b$ (see Fig. 1). We introduce two dimensionless coordinates, namely the slow coordinates x_i, $i = 1,2,3$, and the fast coordinates $\xi_i = x_i/\alpha$, $i = 1,2,3$, where the parameterα is given by b/L. The relaxation tensors are functions of the coordinates since it is assumed they depend on ξ_i, $i = 1,2,3$.

In the linear theory of viscoelasticity, the constitutive law can be written in the

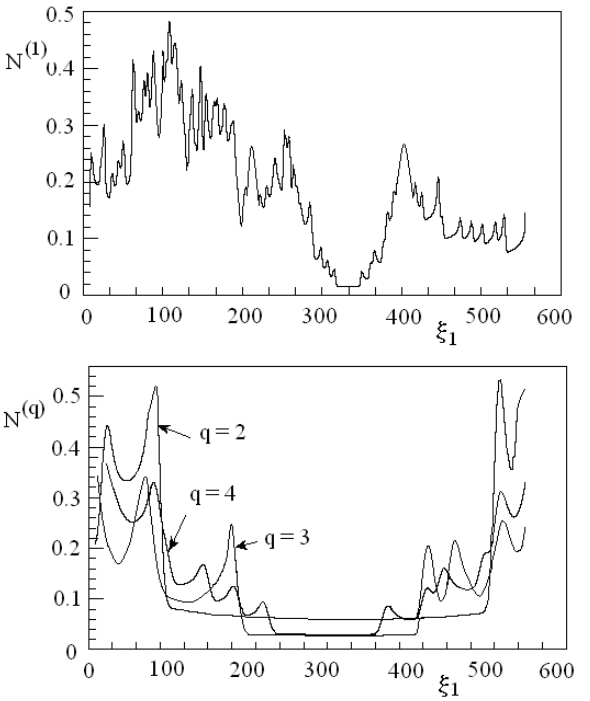

Figure 1: Elementary cell with integrated carbon nanotube film.

following form

$$\sigma_{ij} = \int_0^t R_{ijkl}(x,t-\tau)\mathrm{d}\varepsilon_{kl}(\tau) \equiv \check{R}_{ijkl}(x)\varepsilon_{kl}, \quad i,j,k,l = 1,2,3, \tag{2.1}$$

$$\sigma_{ij} = \int_0^t R_{ijkl}(x,t-\tau)\mathrm{d}\varepsilon_{kl}(\tau) \equiv \check{R}_{ijkl}(x)\varepsilon_{kl}, \quad i,j,k,l = 1,2,3, \tag{2.2}$$

where σ_{ij} are the stress tensor components, ε_{kl} are the strain tensor components, $R_{ijkl}(x,t-\tau)$ are the relaxation kernel tensor components which depend on the spatial, x, and temporal, t, variables,

$$R_{ijkl}(x,t) = \lambda(x,t)\delta_{ij}\delta_{kl} + \mu(x,t)(\delta_{ik}\delta_{jl} + \delta_{il}\delta_{jk}), \quad i,j,k,l = 1,2,3. \tag{2.3}$$

Here $\lambda(t-\tau)$ and $\mu(t-\tau)$ are the stress-relaxation Lamé functions. The tensors $R_{ijkl}(x,t-\tau)$ satisfy the following symmetry conditions [Pobedria (1995)]

$$R_{ijkl} = R_{jikl} = R_{ijlk} = R_{klij}, \quad i,j,k,l = 1,2,3. \tag{2.4}$$

The effective relaxation kernel tensor $\check{R}_{ijkl}(x)$ depends only on x and is given by

$$\check{R}_{ijkl}(x) = \check{\lambda}(x)\delta_{ij}\delta_{kl} + \check{\mu}(x)(\delta_{ik}\delta_{jl} + \delta_{il}\delta_{jk}), \quad i,j,k,l = 1,2,3, \tag{2.5}$$

The constitutive law can be written in the inverse form

$$\varepsilon_{ij} = \int_0^t J_{ijkl}(x,t-\tau)\mathrm{d}\sigma_{kl}(\tau) \equiv \check{J}_{ijkl}(x)\sigma_{kl}, \quad i,j,k,l = 1,2,3, \tag{2.6}$$

where $J_{ijkl}(x,t-\tau)$ are the creep kernel tensor components which depend on the spatial x and temporal t variables, and $\check{J}_{ijkl}(x)$ is the effective creep kernel tensor which depends on x only.

The equation on motion in the absence of body forces can be written as

$$[\check{R}_{ijkl}u_{k,l}]_{,j} - \rho\ddot{u}_i = 0, \quad i,j,k,l = 1,2,3, \tag{2.7}$$

where ρ is the mass density of the body. Boundary and initial conditions should be prescribed, namely

$$u_i|_{\Sigma_1} = u_i^0, \quad \check{R}_{ijkl}u_{k,l}|_{\Sigma_2} = S_i^0, \quad i,j,k,l = 1,2,3, \quad \forall t, \quad u_i|_{t=0} = u_{i0}^0, \quad \dot{u}_i|_{t=0} = u_{pi0}^0 \tag{2.8}$$

where u_i^0, S_i^0, u_{i0}^0 and u_{pi0}^0 are known quantities.

The generalized Cosserat theory is obtained from Eqs. (2.1)-(2.5) by introducing the couple-stresses into the constitutive equations of the linear theory of viscoelasticity. In addition to the stress tensorσ_{ij},$\sigma_{ij} \neq \sigma_{ji}$, the couple-stress tensor $\mu_{ij} \neq \mu_{ji}$ is introduced, and to the displacement vector components u_i, which are related to the strain components by $\varepsilon_{ij} = 1/2\,(u_{i,j} + u_{j,i})$, the rotation vector (spin-vector) components $\omega_i = u_{k,l}\varepsilon_{ikl}$ are also introduced. The curvature tensor is the gradient of ω_i. The components$\kappa_{ij}$of the curvature tensor are given by

$$\omega_{i,j} = u_{k,lj}\varepsilon_{ikl} = \kappa_{ij}, \quad i,j = 1,2,3, \tag{2.9}$$

with $e_i$the orthonormal basis of the coordinate system.

By generalizing relation (2.1), the constitutive laws can be represented as [Pobredia (1998)]

$$\sigma_{ij} = \check{S}_{ijkl}u_{k,l} + \check{s}_{ijkl}\kappa_{kl}, \quad \mu_{ij} = \check{D}_{ijkl}u_{k,l} + \check{E}_{ijkl}\kappa_{kl}, \tag{2.10}$$

where new unknown material functions are introduced, namely the relaxation tensors $\check{S}_{ijkl}$, $\check{s}_{ijkl}$, $\check{D}_{ijkl}$ and $\check{E}_{ijkl}$. These tensors do not satisfy the symmetry property (2.2).

By using Eq. (2.6), the constitutive laws (2.7) become

$$\sigma_{ij} = \check{S}_{ijkl}u_{k,l} + \check{s}_{ijkl}u_{m,nl}\varepsilon_{kmn}, \quad \mu_{ij} = \check{D}_{ijkl}u_{k,l} + \check{E}_{ijkl}u_{m,nl}\varepsilon_{kmn}. \tag{2.11}$$

The equation of motion (2.4) in the absence of body forces and body couples recasts as

$$\sigma_{ji,j} - \rho\ddot{u}_i = 0, \quad \mu_{ji,j} + \varepsilon_{ijk}\sigma_{jk} - \rho\, j\ddot{\omega}_i = 0, \tag{2.12}$$

where j is the microinertia. We mention that σ_{ji}, μ_{ji} can be expressed by using Eq. (2.7) in terms of the displacements u_i, $i = 1,2,3$.

Then the boundary and initial conditions (2.5) become

$$u_i|_{\Sigma_1} = u_i^0, \quad \sigma_{ij}|_{\Sigma_2} = S_i^0, \quad \omega_i|_{\Sigma_1} = \omega_i^0, \quad \mu_{ji}n_j|_{\Sigma_2} = M_i^0, \quad \forall t, \tag{2.13}$$

$$u_i|_{t=0} = u_{i0}^0, \quad \dot{u}_i|_{t=0} = u_{pi0}^0,$$

where u_i^0, S_i^0, ω_i^0, M_i^0, u_{i0}^0 and u_{pi0}^0 are known quantities.

The couple-stress tensor components μ_{ij} depend on the stresses and the structure of the composite. Therefore, according to the method of Pobedria and Omarov (2007b), we introduce the following relation

$$\mu_{ij} = \sigma_{ik}\varepsilon_{lkj}\varphi_l(\xi_1,\xi_2,\xi_3), \tag{2.14}$$

where the vector φ specifies the structure of the composite beam [Pobedria and Omarov (2007a)]

$$\varphi_i(\xi_1,\xi_2,\xi_3) = \alpha\xi_i(1+\alpha a_j\xi_j+\alpha^2 b_{jk}\xi_j\xi_k+...), \tag{2.15}$$

and $a_j, b_k, ...$ are known quantities.

3 Homogenenization technique

The problem (2.9) and (2.10) is solved by the homogenization method discussed by Pobedria (1984). The generalized solution to this problem is sought in the following form $u_i(x_1,x_2,x_3,t) = U_i(x_1,x_2,x_3)\exp(\mathrm{i}\check{\omega}t)$, where $\check{\omega}$ is the frequency. For $U_i(x_1,x_2,x_3)$, we chose the asymptotic expansion of the qth level with respect to the small parameter α

$$U_i = v_i + \alpha\check{N}^{(1)}_{ijk_1}v_{j,k_1} + \alpha^2\check{N}^{(2)}_{ijk_1k_2}v_{j,k_1k_2} + ...\alpha^q\check{N}^{(q)}_{ijk_1...k_q}v_{j,k_1...k_q}, \quad q=0,1,..., \tag{3.1}$$

where $v_i(x_1,x_2,x_3)$, $i=1,2,3$ are the components of the displacement vector for the reduced medium, $\check{N}^{(q)}_{ijk_1...k_q}(\xi_1,\xi_2,\xi_3)$ are the local relaxation kernels of the qth level. These kernels are periodic in (ξ_1,ξ_2,ξ_3) and satisfy the following conditions

$$N^{(0)}_{ij} \equiv \delta_{ij}, \quad N^{(q)}_{ijk_1...k_q} = 0 \text{ for } q<0, \quad \left\langle N^{(q)}_{ijk_1...k_q}\right\rangle = 0 \text{ for } q>0. \tag{3.2}$$

where we have denoted by $\langle f\rangle$ the homogenization operator applied to a function f with respect to the variables (ξ_1,ξ_2,ξ_3).

The expansion (3.1) is used to express the stresses (2.1) and the couple-stresses (2.11) in terms of displacements and rotations. By substituting Eq. (3.1) into Eqs. (2.9) and (2.10) we obtain two sequences; more precisely, one of the aforementioned sequences is used for finding$v_i(x_1,x_2,x_3,t)$, while the second one is employed for retrieving the local relaxation kernel$\check{N}^{(q)}_{ijk_1...k_q}(\xi_1,\xi_2,\xi_3)$.

If the local relaxation functions $\check{N}^{(q)}_{ijk_1...k_q}(\xi_1,\xi_2,\xi_3)$ are known then the effective relaxation tensors can be calculated by

$$h^{(q)}_{ijkl_1...l_{q+1}} = \left\langle \check{R}_{ijml_{q+1}}N^{(q)}_{mkl_1...l_q} + \check{R}_{ijmn}N^{(q+1)}_{mkl_1...l_{q+1}|n}\right\rangle, \quad q=0,1,... \tag{3.3}$$

where the derivative with respect to the fast variables ξ_i, $i=1,2,3$, is denoted by $f_{|i}$.

Substituting the asymptotic expansion

$$v_i = \sum_{p=0}^{\infty} w_i^p, \tag{3.4}$$

into Eq. (3.1), we obtain

$$U_i = \sum_{p=0}^{\infty} w_i^p + \sum_{q=0}^{\infty} \alpha^q \sum_{p=0}^{q} \check{N}^{(p)}_{ijk_1\ldots k_p} w^{(q-p)}_{j,k_1\ldots k_p}. \tag{3.5}$$

Thus, the problem (2.9) and (2.10) can be reduced to two recurrent sequences of problems. The first sequence related to the original problem consists of solving the following boundary value problems associated with the linear viscoelastic theory for anisotropic homogeneous media

$$\check{h}^{(0)}_{ijlk_1} w^{(p)}_{l,k_1 j} - \rho \sum_{p=0}^{\infty} \left(\ddot{w}_i^p + \check{N}^{(p)}_{ijk_1} \ddot{w}^{(p)}_{j,k_1} \right) = 0, \quad w_i^{(p)}|_{\Sigma_1} = u_i^{(p)}, \quad \check{h}^{(0)}_{ijlk_1} w^{(p)}_{l,k_1} n_j|_{\Sigma_2} = S_i^{(p)} \tag{3.6}$$

The input data are defined by

$$S_i^{(p)} = -\sum_{q=1}^{p} h^{(q)}_{ijlk_1\ldots k_{q+1}} w^{(p-q)}_{l,k_1\ldots k_{q+1}} n_j|_{\Sigma_2} \text{ for } p>0, \quad S_i^{(p)} = S_i^0 \text{ for } p=0, \tag{3.7}$$

and

$$u_i^{(p)} = -\sum_{q=1}^{p} N^{(q)}_{ijlk_1\ldots k_q} w^{(p-q)}_{j,k_1\ldots k_q}|_{\Sigma_1} \text{ for } p>0, \quad u_i^{(p)} = u_i^0 \text{ for } p=0, \tag{3.8}$$

where $h^{(q)}_{ijlk_1\ldots k_{q+1}}$ are the components of the effective relaxation tensor of the qth level with $h^{(q)}_{ijlk_1\ldots k_{q+1}} \equiv 0$ for $q<0$.

The relaxation tensor $h^{(q)}_{ijlk_1\ldots k_{q+1}}$ is determined from the second sequence related to the original problem, which consists of solving the following boundary value problems associated with the linear viscoelastic theory for an inhomogeneous medium with periodic cells, i.e.

$$\left(\check{R}_{ijml} N^{(q+2)}_{mnk_1\ldots k_{q+2|l}}\right)_{|j} + \left(\check{R}_{ijmk_{q+2}} N^{(q+1)}_{mnk_1\ldots k_{q+1}}\right)_{|j} + \check{R}_{ik_{q+2}ml} N^{(q+1)}_{mnk_1\ldots k_{q+1|l}} + \check{R}_{ik_{q+2}mk_{q+1}} N^{(q)}_{mnk_1\ldots k_q} = h^{(q)}_{ik_{q+2}nk_1\ldots k_{q+1}}. \tag{3.9}$$

The unknown relaxation tensors $\check{S}_{ijkl}$, $\check{s}_{ijkl}$, $\check{D}_{ijkl}$ and $\check{E}_{ijkl}$ of the constitutive laws (2.8) cannot be studied experimentally, however they can be found by this homogenization method [Pobedria and Omarov (2007a)].

For the zeroth- and first-order approximation theories, it is sufficient to consider only one or two problems in each of the recurrent sequences. When the first two local functions $N^{(1)}_{ijk_1}$ and $N^{(2)}_{ijk_1}$ are found, the zeroth- and first-order approximation theories give

$$\check{S}_{ijkl} = \check{R}_{ijmn}N^{(1)}_{mkl|n} + R_{ijkl}, \quad \check{s}_{ijkl} = -2\alpha\varepsilon_{nmk}(\check{R}_{ijps}N^{(2)}_{pnml|s} + \check{R}_{ijpl}N^{(1)}_{pnm}),$$

$$\check{D}_{ijkl} = \varepsilon_{jnm}\varphi_m(\check{R}_{inpq}N^{(1)}_{pkl|q} + R_{inkl}), \quad \check{E}_{ijkl} = -2\alpha\varepsilon_{qpj}\varphi_q(\check{R}_{ipms}N^{(2)}_{pnml|s} + \check{R}_{ipml}N^{(1)}_{mnr})\varepsilon_{nrk}, \tag{3.10}$$

with φ_k defined by Eq.(2.12).

Therefore, for the zeroth- and first-order approximation theories, the material functions $\check{S}_{ijkl}$, $\check{s}_{ijkl}$, $\check{D}_{ijkl}$ and $\check{E}_{ijkl}$ can be expressed by Eq. (3.10) with respect to R_{ijkl},$\check{R}_{ijmn}$, $N^{(1)}_{mkl}$, $N^{(2)}_{pnml}$, φ_q and α, with no additional experimental tests.

4 Results

Consider a reinforced carbon nanotube beam cantilevered at the root and excited by the piezoelectric sheet with a sinusoidal control voltage. The present computations were carried out for the same sandwich beam tested experimentally by Koratkar *et al.*, namely L =22.86mm, a =25.4mm, b =0.91mm, h_1 =0.61mm, h_2 =0.05mm, h_3 =0.25mm. The piezo-induced strain generates a cross-sectional bending moment resulting in the flat-wise bending deformation. The PZT-SH is characterized by the Young's modulus E =69GPa and the density ρ =7.8g/cm^3. For Silica the Young modulus is E =131GPa and the density is given by ρ =2.33 g/ cm^3. The nanofilm is composed of multiwalled nanotubes and epoxy and it is characterized by the Young modulus$E$ = 284GPa and the density ρ =1.1 g/cm^3.

Herein we use Voigt's convention to denote each pair of indexes of the elastic constants by a single index, namely

$$(i, j) \to i\delta_{ij} + (9 - i - j)(1 - \delta_{ij}).$$

According to this convention we have $\check{M}_{klmn} = \check{M}_{\alpha\beta}$ (for $\check{R}_{ijmn}$, R_{ijkl}, $\check{S}_{ijkl}$, $\check{s}_{ijkl}$, $\check{D}_{ijkl}$ and $\check{E}_{ijkl}$) where the Latin subscripts range over the values 1,2,3, while the Greek subscripts range over the values 1,2,...,6. The components σ_{kl} and ε_{kl} are replaced by $\sigma_{kl} = \sigma_\alpha$, $2\varepsilon_{kl}(1 + \delta_{kl}) = \varepsilon_\alpha$, $k, l = 1, 2, 3$, $\alpha = 1, 2, ...6$. So, we have

$$\check{R}_{11} = \check{R}_{23} = \check{\lambda}(\xi) + 2\check{\mu}(\xi), \quad \check{R}_{12} = \check{R}_{13} = \check{R}_{23} = \check{\lambda}(\xi),$$

$$\check{R}_{33} = \check{R}_{44} = \check{R}_{55} = \check{R}_{66} = \check{\mu}(\xi).$$

In Fig. 1 we plot the variation of the local normalized relaxation function $N^{(q)} = \check{N}^{(q)}_{ijk_1\ldots k_q}/\check{N}^{(1)}_{ijk_1}$ with respect to ξ_1, for $i=j=k=1$ and $q=1,2,3,4$ for a cantilevered beam. The function $N^{(1)}$ exhibits a short sudden decrease of its value in the vicinity of ξ_1 =333. The curve becomes flat for $N^{(2)}$ with a decrease of its value from approximately ξ_1 =120 to ξ_1 =570. For $q=3$ and $q=4$ the flat curves are shorter than those for the case discussed above, but larger than those obtained for $q=1$. The variation of the local relaxation functions seems to give information about the properties of the effective material functions$\check{S}_{\alpha\beta}$,$\check{s}_{\alpha\beta}$,$\check{D}_{\alpha\beta}$ and $\check{E}_{\alpha\beta}$. These functions calculated for $\alpha=\beta=1$ are presented in Fig. 2. It can be seen from this figure that the values of these functions have a flat zone in the vicinity of ξ_1 =300.

The Young's modulus of the composite is a measure of the stiffness against small axial stretching and compression strains, as well as non-axial bending and torsion strains on the beam.

This is expressed as $\check{E}(x) = \frac{(3\check{\lambda}+2\check{\mu})\check{\mu}}{\check{\lambda}+\check{\mu}}$. The axial elastic modulus of the beam is calculated from the second derivatives of the potential energy functional with respect to the axial strain $Y = -\frac{1}{V}\Pi_{,\varepsilon\varepsilon}$ [Chen, Cheng and Hsu (2007)].

$$\Pi = \frac{1}{2}\int_V (\check{S}_{ijkl}+\check{D}_{ijkl})\varepsilon_{kl}\varepsilon_{ij}\mathrm{d}V + \frac{1}{2}\int_V (\check{s}_{ijkl}+\check{E}_{ijkl})\kappa_{kl}\kappa_{ij}\mathrm{d}V - \int_{\partial V} t_i u_i d\Sigma - \int_{\partial V} q_i \omega_i d\Sigma.$$

where $t_i = \sigma_{ij}n_j$ is the traction vector, $q_i = \mu_{ij}n_j$ is the couple tractions vector and n_i is the outward unit normal vector to the surface.

A relevant result is shown in Fig. 3, where the variation of the Young's modulus with respect to b is plotted in comparison with the classical Young's modulus. We find that the modulus is higher than that of the Silica and PZT-SH materials. These results indicate an increase in Young's modulus of up to 18.8% in comparison with the classical theory.

We have also performed computations for the dynamic trajectories of the rotation vector (spin-vector). The phase portrait of the components ω_1 and ω_2 in the plane(ξ_1,ξ_3) is plotted in Fig. 4. The spiraling behavior of the spin trajectories suggests the effect of the relaxation properties and the existence of a stable circular orbit. This stable limit cycle attracts all neighboring trajectories. As a consequence, the beam can exhibit self-sustained spin oscillations.

In order to compare the present results with the experimental ones of Koratkar, Wei and Ajayan (2003), we calculate the response of the cantilevered beam for a frequency test (50 Vrms voltage input to the piezoelectric sheet). Fig.5 compares the variation of the root microstrain with respect to the frequency for the no reinforced and reinforced cases. Both the baseline and the CNT-reinforced beams have

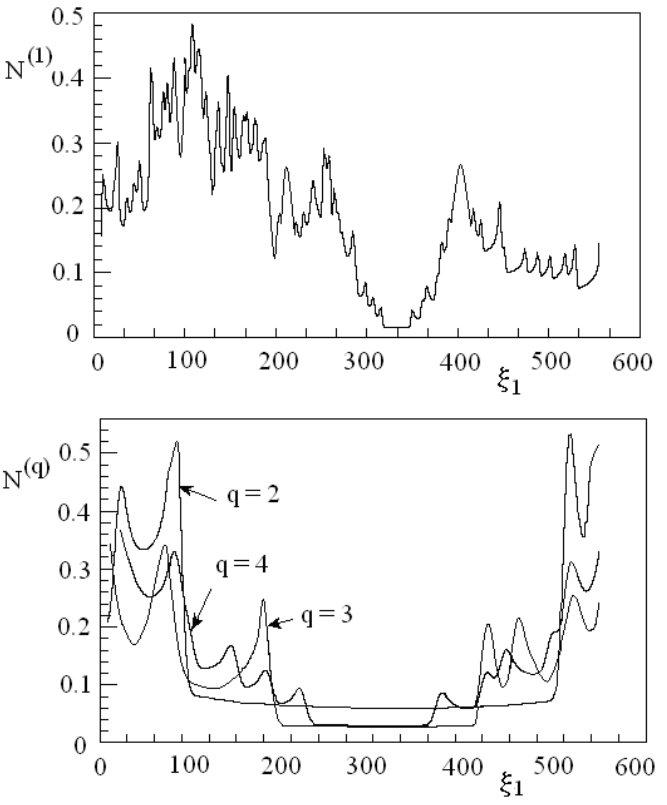

Figure 2: Variation of the local normalized relaxation functions with respect to ξ_1 for $q = 1,2,3,4$.

the same cross-sectional dimensions (25.4mm$\times$0.91mm) and cantilevered length (22.86mm). These results are comparable to those obtained using the Koratkar experimental data, indicating a significant decrease in the root microstrain (about 25%) with increasing frequency.

Fig. 6 presents the variation of the root microstrain with respect to the frequency for the clamped beam with and without carbon nanotube reinforcement. A significant decrease in the root microstrain (about 25%) with increasing frequency is also found.

Fig. 7 presents snapshots of various shapes of the deformed carbon nanotube clamped beam and excited by the piezoelectric sheet with a sinusoidal voltage.

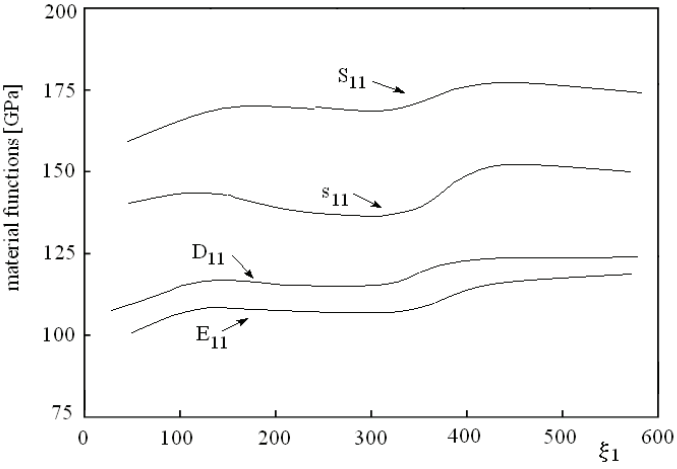

Figure 3: Variation of the material functions $\check{S}_{11}$, $\check{s}_{11}$, $\check{D}_{11}$ and $\check{E}_{11}$ with respect to ξ_1.

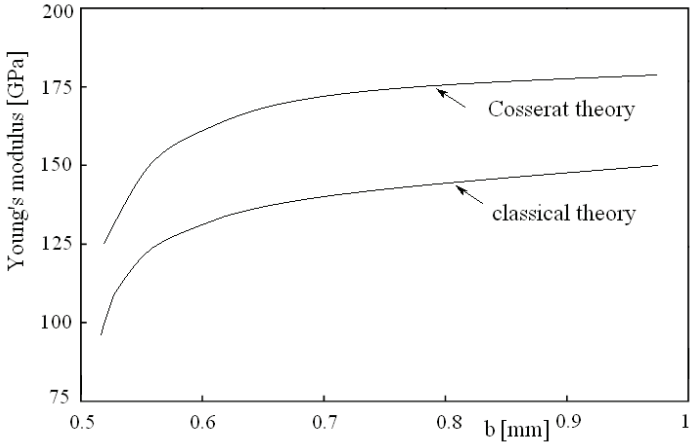

Figure 4: Variation of the Young's modulus with respect to b in comparison to the classical modulus.

5 Conclusions

Carbon nanotubes are attractive for the structural reinforcement because they can potentially be integrated within composites and offer multifunctionality in terms of

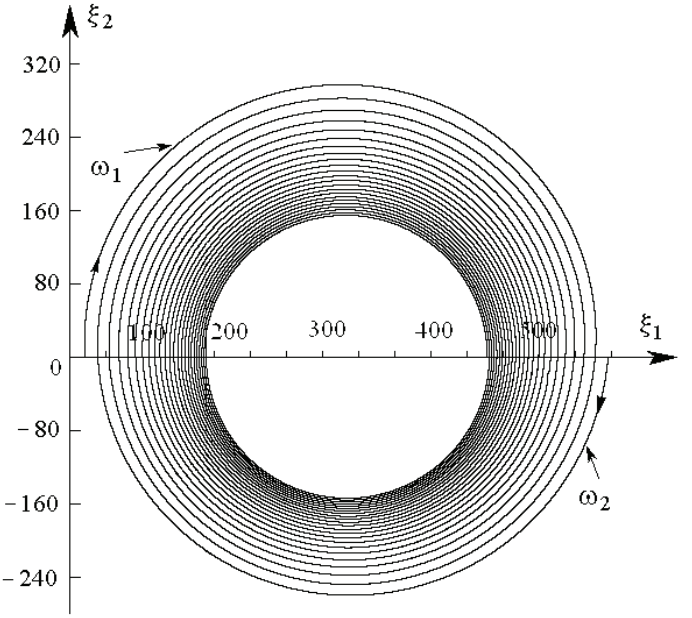

Figure 5: Trajectories of the spin component ω_1 and ω_2.

improved damping, stiffness, strength, and fracture toughness.

The model of the sandwich beam presented in this paper was obtained by introducing the couple-stresses into the constitutive equations of the linear viscoelastic theory. The effective material functions were calculated, in the framework of the zeroth- and first-order approximation theories, from the local relaxation tensors by a homogenization method, without the requirement of additional experimental tests. The variation of the beam root microstrain was compared with the bending experimental results reported by Koratkar *et al.* (2003). The results presented in this study showed an enhancement in both the structural damping and stiffness of this composite beam due to the nanotube reinforcement.

Acknowledgement: This research was financially supported by the National Authority for Scientific Research (ANCS, UEFISCSU), Romania, through the PN2 Project 106/2007, CNCSIS code 247/2007. The authors would like to extend their sincere thanks to Dr. Liviu Marin for his help in preparing this paper.

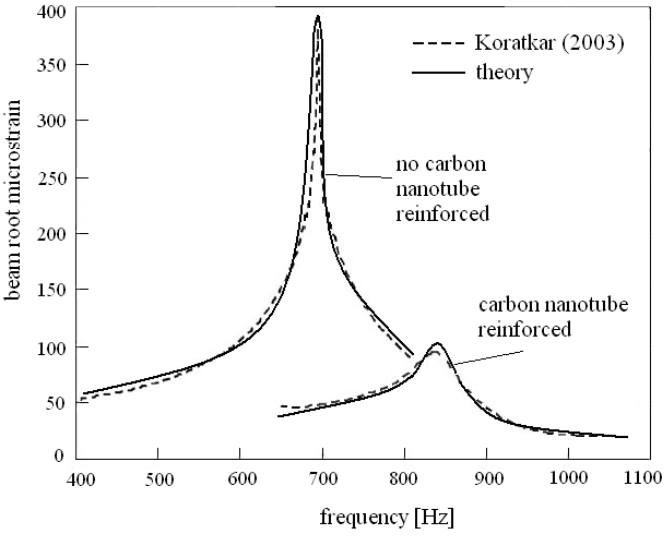

Figure 6: Variation with respect to frequency of the root microstrain for the cantilevered baseline and the nanotube reinforced beams.

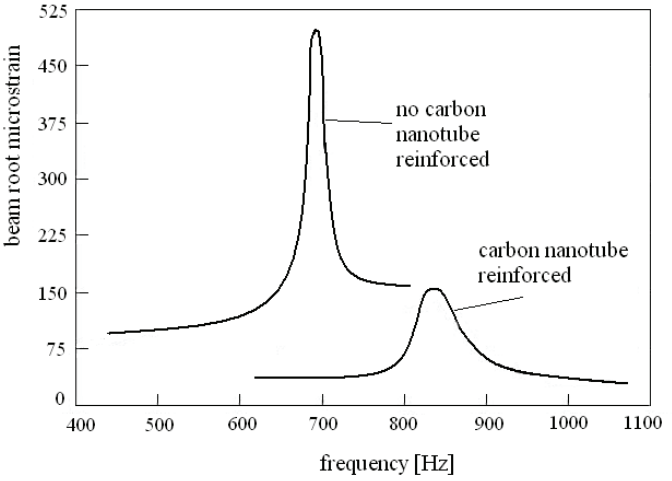

Figure 7: Variation with respect to frequency of the root microstrain for the clamped baseline and the nanotube reinforced beams.

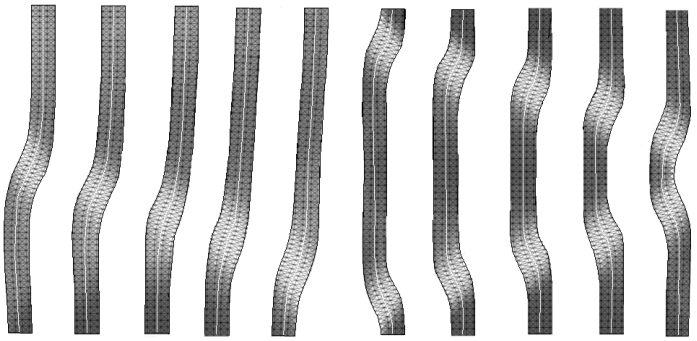

Figure 8: Snapshots of various shapes of the deformed clamped beam.

References

Biggerstaff, J.; Kosmatka, J. (1998): Damping performance of cocured viscoelastic composite laminates with embedded viscoeleastic layers. *Journal of Composite Materials* 32(21).

Brackbill, C.; Ruhl L.; Lesieutre, G.; Smith, E. (2000): Characterization and modeling of the low strain amplitude and frequency dependent behavior of elastomeric damper materials. *Journal of the American Helicopter Society* 45(1): 34–42.

Brenner, D. W.; Shenderova, O. A.; Areshkin, D. A.; Schall, J. D.; Frankland, S.J.V. (2002): Atomic modeling of carbon-based nanostructures as a tool for developing new materials and technologies. *CMES: Computer Modeling in Engineering & Science* 3(5): 643–673.

Calvert, P.: (1992): Materials science-strength in disunity. *Nature* 357(6377):365–366.

Chakrabarty, A.; Cagin, T. (2008): Computational studies on mechanical and thermal properties of carbon nanotube based nanostructures. *CMC: Computers Materials & Continua* 7(3): 167–189.

Chen, W.H.; Cheng, H.C.; Hsu, Y.C. (2007): Mechanical Properties of Carbon Nanotubes Using Molecular Dynamics Simulations with the Inlayer van der Waals Interactions. *CMES: Computer Modeling in Engineering & Sciences* 20(2): 123–145.

Cheng, H.C.; Hsu, Y.C.; Chen, W.H. (2009): The Influence of Structural Defect on Mechanical Properties and Fracture Behaviors of Carbon Nanotubes. *CMC: Computers, Materials and Continua* 11(2): 127–146.

Chiroiu, V.; Munteanu. L. ; Donescu, St. (2006): On the mechanical modeling of single-walled carbon nanotubes. *Rev. Roum. Sci,. Techn., serie Mécanique Appl.* 51(1): 37–52.

Chiroiu, V.; Munteanu, L.;Paun, V.P.; Teodorescu, P.P. (2009): On the Bending and Torsion of Carbon Nanotubes Ropes, *New Applications of Micro- and Nanotechnologies, Series of Micro and Nanoengineering.* 14: 26–44,

Cosserat, E.F.; Cosserat, F.F. (1909): *Théorie des corps déformables*, Hermann et Fils, Paris. Engl. Transl.of the title: Theory of Deformable Bodies.

Giannopoulos, G.I.; Georgantzinos, S.K.; Katsareas, D.E.; Anifantis, N.K. (2010): Numerical prediction of Young's and shear moduli of carbon nanotube composites Incorporating Nanoscale and interfacial effects. *CMES: Computer Modeling in Engineering & Sciences* 56(3): 231–248.

Koratkar, N.A.; Wei, B.; Ajayan, P.M. (2003): Multifunctional structural reinforcement featuring carbon nanotube films. *Composites Science and Technology* 63: 1525–1531

Li, C.Y.; Chou T.W. (2003): Elastic moduli of multi-walled carbon nanotubes and the effect of van der Waals forces. *Composites Science and Technology* 63: 1517–1524.

Liao, W.; Wang K. (1997): On the analysis of viscoelastic materials for active constrained layer damping treatments. *Journal of Sound and Vibration* 207(3): 319–334.

Maly, J.; Johnson C. (1996): Cocured viscoelastic composites. *SPIE Smart Structures and Materials Conference Proceedings*, San Diego, CA, USA, 365–376.

Munteanu, L.; Chiroiu, V. (2009): Shell Buckling of Carbon Nanotubes Using Nanoindentation. *CMES: Computer Modeling in Engineering & Science* 48 (1): 27–41.

Nair, A.K.; Farkas, D.; Kriz, R.D. (2008): Molecular Dynamics Study of Size Effects and Deformation due to Nanoindentation. *CMES: Computer Modeling in Engineering & Sciences* 24(3): 239–248.

Nasdala, L.; Ernst G.; Lengnick, M.; Rothert, H. (2005): Finite Element Analysis of Carbon Nanotubes with Stone-Wales Defects, *CMES: Computer Modeling in Engineering & Sciences* 7(3): 293–304.

Overney, G.; Zhong, W.; Tomanek, D.Z. (1993): Structural rigidity and low frequency vibrational-modes of long carbon tubules. *Z. Phys. D.* 27(1): 93–96.

Pobedria, B.E.; Omarov, S.E. (2007a): Determination of material functions for the linear moment theory of viscoelasticity. *Moscow University Mechanics Bulletin* 62(5): 117–122.

Pobedria, B.E.; Omarov, S.E. (2007b): Constitutive relations in the moment theory of elasticity. *Vestn. Mosk. Univ., Ser.1: Mat. Mekh.* 3: 57–59.

Pobedria, B.E. (1998): On damage models of rheonomic media. Izv. Ross. *Akad. Nauk, Mekh. Tverd. Tela*, 4: 128–148 [Mech. Solids 33 (4), 108–124.

Pobedria, B.E. (1995): Numerical methods in the theory of elasticity and plasticity. *Mosk. Gos. Univ. Moscow* (in Russian).

Pobedria, B.E. (1984): Mechanics of composite materials. *Mosk. Gos. Univ. Moscow* (in Russian).

Robertson, D.H.; Brenner, D.W.; Mintmire, J.W. (1993): Energetics of nanoscale graphitic tubules. *Phys. Rev. B.* 45(21): 12592–12595

Ru, C.Q. (2001): Axially compressed buckling of a doublewalled carbon nanotube embedded in an elastic medium. *J. of Mechanics and Physical Solids*, 49: 1265–1279.

Shen, S.; Atluri, S.N. (2004): Computational Nano-Mechanics and Multi-scale Simulation. *CMC: Computers, Materials, & Continua.* 1(1), 59–90.

Solano C.J.F.; Costales A.; Francisco E.; Pendáas A.M.; Blanco M.A.; Lau K.C.; He H., Pandey R. (2008): Buckling in Wurtzite-Like AIN Nanostructures and Crystals: Why Nano can be Different. *CMES: Computer Modeling in Engineering & Sciences* 24(2): 143–156.

Srivastava, D.; Atluri, S.N. (2002): Computational Nano-technology: A Current Perspective. *CMES: Computer Modeling in Engineering & Sciences* 3(5): 531–538.

Theodosiou, T.C.; Saravanos, D.A. (2007): Molecular Mechanics Based Finite Element For Carbon Nanotube Modeling. *CMES: Computer Modeling in Engineering & Sciences* 19(2): 121–134.

Teodorescu, P.P.; Munteanu, L.; Chiroiu, V.; Dumitriu, D.; Beldiman, M. (2008): On the application of Chebyshev polynomials to nanoropes twist. *Proc. of the Romanian Academy, Series A: Mathematics, Physics, Technical Sciences, Information Science*, 9(3): 209–215. ‘.

Voigt, W. (1887): Theoretische Studien über die Elasticitatsverhaltnisse der Krystalle. *Abh. Ges. Wiss.* Göttingen 34.

Xie, G.Q.; Long, S.Y. (2006): Elastic Vibration Behaviors of Carbon Nanotubes based on Micropolar Mechanics. *CMC: Computers, Materials and Continua* 4(1): 11–19.